Elsevier Editorial System(tm) for Materials Science & Engineering A
Manuscript Draft

Manuscript Number: MSEA-D-09-02398R1

Title: Interfacial Fracture Behavior of Tungsten Wire/Tungsten Matrix Composites with Copper-Coated Interfaces

Article Type: Research Paper

Keywords: tungsten composites, toughness, fiber-reinforced composites, fiber push-out test, interface debonding, plasma-facing material

Corresponding Author: Dr. Jeong-Ha You, Dr.-Ing.

Corresponding Author's Institution: Max-Planck-Institute of Plasma Physics

First Author: Juan Du, MSc.

Order of Authors: Juan Du, MSc.; Till Höschen1, Dipl.-Ing.; Marcin Rasinski, MSc.; Jeong-Ha You, Dr.-Ing.

Abstract: The potential application of tungsten as a structural material has been strongly restricted by inherent brittleness. The hitherto metallurgical efforts to improve tungsten toughness seem to be still less matured. The authors have been exploring a novel toughening technique based on reinforcement by tungsten wires. Toughness is supposed to be enhanced through the energy dissipation at the wire/matrix interfaces which is caused by the controlled crack deflection and friction. In this work, we focus on two kinds of copper coatings for interface engineering, namely, copper mono-layer and copper/tungsten multi-layer. Single filament composites were fabricated using magnetron sputtering and CVD process. The interfacial parameters were identified by means of fiber push-out test and microscopic fracture features were investigated. In this paper the results from the extensive push-out experiments are presented together with the fractographs. Finite element simulation was also carried out to estimate the plastic strain of the copper layer. Essential role of the significant plastic deformation in the overall failure behavior is highlighted.

Response to the reviewers

Reviewer1.

The text paragraph was revised according to the reviewer's recommendation (many thanks). The corresponding references were updated [1, 2] and replaced [4].

Reviewer2.

1) The manufacturing of the many filament bulk W/W composite materials is a current Ph.D thesis topic of one of my students (since 1 year). This highly challenging study treats the processing development including compaction.

2) A direct quantitative comparison of the dissipated energy was added in page 6 line 9-12.

3) Still we could not give a general statement about the correlation between ductility of the interface and shear strength, because our experimental result was obtained only for specific ad hoc case of Cu and Cu/W coating layers. We were not sure if metallurgical effects (bonding, wetting, roughness etc.) would have possibly played a more dominant role than the continuum mechanical factors.

4) Figure 5 was improved. Figure 1 was explained in detail.

5) All English corrections were made (many thanks).

Response to the editor

The mathematical equation was re-typed in according to the instruction. The revised text parts were marked in blue color.

Interfacial Fracture Behavior of Tungsten Wire/Tungsten Matrix Composites with Copper-Coated Interfaces

J. Du[1], T. Höschen[1], M. Rasinski[1,2], J-H. You[1*]

[1] Max-Planck-Institut für Plasmaphysik, EURATOM Association,
Boltzmannstr. 2, 85748 Garching, Germany

[2] Warsaw University of Technology, Faculty of Materials Science and Engineering,
ul. Woloska 141, 02-507 Warsaw, Poland

Abstract

The potential application of tungsten as a structural material has been strongly restricted by inherent brittleness. The hitherto metallurgical efforts to improve tungsten toughness seem to be still less matured. The authors have been exploring a novel toughening technique based on reinforcement by tungsten wires. Toughness is supposed to be enhanced through the energy dissipation at the wire/matrix interfaces which is caused by the controlled crack deflection and friction. In this work, we focus on two kinds of copper coatings for interface engineering, namely, copper single-layer and copper/tungsten multi-layer. Single filament composites were fabricated using magnetron sputtering and CVD process. The interfacial parameters were identified by means of fiber push-out test and microscopic fracture features were investigated. In this paper the results from the extensive push-out experiments are presented together with the fractographs. Finite element simulation was also carried out to estimate the plastic strain of the copper layer. Essential role of the significant plastic deformation in the overall failure behavior is highlighted.

*Corresponding author:
e-mail) you@ipp.mpg.de
Phone) ++49 (0)89 3299 1373
Fax) ++49 (0)89 3299 1212

Keywords: tungsten composites, toughness, fiber-reinforced composites, fiber push-out test, interface debonding, plasma-facing material

1. Introduction

Tungsten is attracting increasing interest in specific high temperature applications, especially as a plasma-facing armor material for fusion reactors, due to its refractory nature, minimal sputtering yield, large heat removal capability and thermal shock resistance. On the other hand, the potential as a structural material is still strongly restricted by its inherent brittleness which prevails below the ductile-to-brittle transition temperature (DBTT). There have been intensive efforts to improve poor tungsten toughness by means of conventional metallurgical methods including alloying with rhenium, severe plastic deformation to form a nano-scale microstructure, mechanical alloying followed by HIP also to form a nano-microstructure, and increase of the degree of deformation (e.g. foils or wires) [1-3]. Oxide particles dispersion could increase the creep strength but reduced the tensile elongation [4]. But it seems very difficult to achieve substantial enhancement in near future despite of the decades of research. Hence, in order to accelerate the progress, one needs to devise a completely novel toughening technique which is not affected by the ductile-to-brittle transition mechanism.

Since mid 1980's, ceramic matrix composites (CMC) reinforced with continuous strong fibers have been developed. In the meantime they were approved as a structural material equipped with extensive global toughness [5, 6]. Numerous experimental studies demonstrated that the long fiber reinforcement could endow the brittle ceramic matrix with significant toughness by interfacial energy dissipation. The effective energy absorption is caused by the controlled crack deflection (debonding) and frictional sliding at the fiber/matrix interfaces [6]. Hence, the fracture energy of the interface plays a key role in this process.

Recently, the authors have been exploring the applicability of this CMC toughening concept for tungsten. To this end, single fiber specimens of tungsten wire-reinforced tungsten matrix composites (W_w/W) were fabricated and investigated by means of fiber push-out test. Their study was focused on the interface engineering using submicron-thick ceramic coatings. The chemical composition of the composites was only minimally changed by the thin coatings. The extensive push-out tests revealed considerable amount of energy dissipation produced by the brittle cracking and frictional sliding of the coated interfaces. In addition, the strength and toughness of the tungsten composite can be further enhanced by the toughness of the tungsten wire itself since the commercially available tungsten wires are normally very strong (2.5~3 GPa) and ductile.

Another possibility to realize the interfacial energy dissipation would be to use a soft metallic coating to exploit substantial plastic deformation. In this work, we discuss the feasibility of

metallic coatings for the interface of the W_w/W composite. First results obtained from the push-out experiments are presented. Two kinds of copper coatings were investigated, namely, copper single-layer and copper/tungsten multi-layers. Interfacial material parameters were identified. The microscopic fracture feature of the debonded interfaces was examined.

2. Experimental procedure

2.1. Specimen preparation

Commercial tungsten wire with diameter of 150 μm was used as reinforcement. The interface coatings were deposited by magnetron sputtering (MS). The single-layer copper coating was 420 nm think, whereas the multi-layer coating consisted of four 55 nm thick copper films and five 110 nm thick tungsten films in an alternating way. The coatings were further coated with a thin tungsten film to protect the surfaces. The coated fibers were then further coated with tungsten using chemical vapor deposition (CVD) at 550°C to form a dense matrix mantle, respectively. As final product, single-filament W_w/W composite rods with a coated interface were fabricated (diameter: 2.5 mm, length: 35mm, filament volume fraction: 0.4%).

Figure 1 and 2 are the scanning electron microscopy (SEM) images of the Cu single-layer and W/Cu multi-layer coating interface in the as-fabricated W_w/W composite, respectively. The longitudinal cross sections were prepared by focused ion beam (FIB). The dark stripes are copper coatings and the bright ones are tungsten. The micrographs exhibited intact adhesion between each coating layer. Energy dispersive X-ray analysis revealed a stepwise profile of chemical concentration at the interfaces indicating negligible inter-diffusion.

The cylindrical rods were carefully sliced using a diamond saw to produce a set of disc-shaped specimens with thickness ranging from 0.05 to 0.3 mm. Both of the cut surfaces were fine-polished. The specimen thickness was limited by the maximum allowed load (<65N) at which cleavage failure of the tungsten carbide indenter punch was caused.

2.2. Testing procedure

The fiber push-out test is the most popular technique to probe the interfacial properties. Load was slowly applied on one cross sectional end of the fiber embedded in the matrix of a sliced composite specimen. The reaction force and the fiber movement are recorded progressively

producing a characteristic load-displacement curve which reveals the debonding strength and frictional resistance of the interface during the push out process.

We used an instrumented macro-indentation system (<2kN) equipped with a load sensing unit, holder positioning table and optical microscope. The configuration of the main push-out testing system is illustrated in Figure 3. The hole diameter of the supporting substrate was 400 μm and the diameter of the indenter punch was 120 μm. The indentation speed was set to 1 μm/s and the time interval between two sampling points was 0.02 seconds. More than 20 specimens were tested for each interface type. Correction was made on the measured curves to eliminate the contribution of the machine compliance which was measured using a stiff tungsten carbide substrate with the same indentation system. The estimated compliance was 1 μm/N. A typical view of a specimen after push-out test is shown in Figure 4. The SEM image shows partly detached copper coating on the pushed-out fiber surface. In order to expose the internal interface for SEM analysis before and after the push-out tests, the base of the pushed-out filament was locally cut out using FIB. Interfacial shear strength τ_d, fracture energy Γ_i, sliding friction stress τ_o and friction coefficient μ were estimated using theoretical models and numerical regression.

3. Results and discussion

3.1. Push-out curve

The measured push-out load vs. fiber-end displacement curves are plotted in Figure 5. The circle markers indicate the interface with the copper single-layer coating whereas the triangles the W/Cu multi-layer coating, respectively. In the initial loading phase the both interfaces showed a nearly linear response until it reached the maximum load P_d (point A). The slopes of the two curves were almost identical. It should be noted that the total displacements include the bending deflection of the whole system as well as the shear strain of the coating layers. The linear load-displacement response may seem to suggest a linear elastic deformation of the overall specimen system. But this interpretation would lead to rather surprising conclusion that the copper films in the single- and multi-layer coatings would have withstood fairly large shearing force without having undergone plastic flow.

The copper coatings were annealed in the CVD fabrication process and thus supposed to be very soft. To clarify the potential plastic flow behavior of the copper coating a finite element

analysis (FEA) was carried out for the single-layer case taking the identical specimen geometry, boundary condition and push-out loading scenario into account. As input data the tensile test data of soft copper were used for the classical J_2 metal plasticity (Prandtl-Reuss model). Commercial FEA code ABAQUS was used. The simulation could be conducted only up to indenter load of 8 N and terminated due to a convergence problem. The Figure 6 and 7 show the simulated load-displacement response in the initial loading phase and the evolution of the cumulative equivalent plastic strain of the copper coating being sheared. The overall load-displacement response exhibited roughly linear development whereas the copper coating began to undergo significant plastic straining already in the early stage. Comparing the two data it is obvious that the apparently linear behavior is actually fully accompanied by the plastic yielding of the copper layer. The validity of this conclusion is however limited by the present size effect. Such a thin copper coating is expected to experience much larger plastic yield strength unlike a usual bulk specimen. It is experimentally well known that the yield stress of copper film increases strongly by several orders of magnitude when the thickness is reduced below micrometer range. This remarkable hardening phenomenon can be explained with severely limited dislocation movement in the thickness direction [7]. If such a size effect should affect the plastic behavior of the copper coating, the amount of accumulated plastic strain would be accordingly reduced by hardening. Unfortunately, more realistic FEA of the plastic strain with consideration of the size effect was not possible, since the corresponding plastic tensile data were not available. On the other hand, the simulation revealed that the total fiber displacement was mostly caused by the shear deformation of the copper interlayer which reached roughly 4% at point A of Figure 5. Thus it might be reasonable to suppose that plastic yield of the copper coating preceded the overall rupture at P_d to some extent.

Contrary to the Cu single-layer, the W/Cu multilayer coating interface exhibited the typical push-out curve of a brittle interface. The characteristic shape of the curve suggests that the capability of plastic flow was strongly restricted by the size effect. The microstructural feature was different as well (to be discussed later).

Beyond the maximum load P_d, the interface coatings exhibited completely different push-out behaviors from each other. The W/Cu multi-layer interface revealed an abrupt load drop due to rapid interfacial debonding triggered by the crack initiation at the free surface edges. This catastrophic debonding may be attributed to the thin-thickness effect. Upon debonding, the stored elastic strain energy was released in sudden bursts leading to dynamic movement of the fiber from A to B until the fiber was fully decelerated by the frictional resistance. The displacement observed during this dynamic event was 28 μm in 40 milliseconds. A slight load

increase is observed from B to C prior to the quasi-static progressive sliding stage. This load jump was needed to overcome the static friction force generated by the interlocking at the ruptured rough interface. After point C, the friction force P_{fr} decreased gradually due to the decreasing contact area.

In the case of the copper single-layer coating the interface displayed a gradual and monotonic decay of the load which maintained a substantial portion of the shear resistance during the push-out sliding stage. The larger area under the curve implies that the copper single layer coating could enable much larger energy dissipation (i.e. absorption of the applied work) than the multi-layer counterpart. The quantity of the dissipated energy after the debonding event could be estimated by integrating the area below each curve. The energy was measured for the same fiber displacement range from 0.01 to 0.08 mm. Its magnitude amounted to 0.0021 J and 0.0014 J for the single- and multi-layer coating case, respectively. The relative difference was more than 30%. This dramatic contrast in the post-debonding response suggests a different mechanism of debonding and sliding.

3.2. Calibration of interfacial parameters

For a quantitative identification of the interfacial shearing resistance, interfacial shear strength τ_d is defined as the maximum average shear stress produced at the interface immediately before it begins to fail. Greszczuk [8] and Lawrence [9] formulated a relationship between the debonding load P_d and the shear strength τ_d based on the shear-lag theory of pull-out test.

$$P_d = \frac{\pi d_f \tau_d}{\alpha} \tanh(\alpha L) \qquad (1)$$

where P_d denotes the applied load at the moment of interface debonding, d_f the fiber diameter, α the shear-lag parameter depending on the elastic properties of the fiber and the matrix, and L is the embedded fiber length. This equation can also be used for the push-out test case for which the embedded length L is replaced by the specimen thickness H. τ_d can be determined by fitting the experimentally measured P_d-H data into this equation.

The collected P_d-H data and fitting result of the both coated interfaces are shown in Figure 8. The debonding strength (i.e. shear strength) of the Cu/W multi-layer interface (429 MPa) is slightly higher than that of the Cu single-layer interface (393 MPa). These τ_d values suggest a moderate shear strength compared to a carbon-coated glass fiber-reinforced cement composite (50 MPa) [10] or a SiC fiber-reinforced titanium composite (500 MPa) [11].

Further important interfacial parameter is the interfacial fracture toughness Γ_i which is defined as the fracture energy under mode II (shear) loading. Liang et al. [12] have developed a model to calibrate Γ_i from a push-out test data which is expressed as

$$p = p_R + 2\sqrt{\frac{\Gamma_i E_f}{B_2 r_f}}e^{\xi} + \frac{\tau_r}{\mu B_1}(e^{\xi} - 1) \qquad (2)$$

where, r_f denotes the fiber radius, p represents the maximum applied stress on the fiber $p = P_d/(\pi r_f^2)$ and $\xi = 2\mu B_1 H/r_f$. B_1 and B_2 denotes dimensionless elastic parameters as follows:

$$B_1 = \frac{\nu_f E_m}{(1-\nu_f)E_m + (1+\nu_m)E_f}, \quad B_2 = 1 - 2\nu_f B_1$$

where ν and E represent the Poisson ratio and the Young's modulus, and the subscripts f and m fiber and matrix, respectively. H denotes the fully embedded fiber length (specimen thickness) and μ the friction coefficient. p_R is the residual axial stress caused by thermal expansion mismatch and thus becomes zero for the W_f/W composite. Γ_i is determined by fitting the experimentally measured $p - H$ data into eq.(2). Since this equation was derived in the framework of elastic fracture mechanics and elastic shear-lag assumption, its validity is limited within small scale yielding case. Thus this approach is less adequate for the copper single-layer coating due to possible plastic straining.

The fitting result for the W/Cu multilayer coating is presented in Figure 9. The calibrated interfacial fracture toughness was 22 J/m². The fact that the quality of the numerical fitting is rather unsatisfactory implies that the present model also has a limited applicability for the W/Cu multilayer coating. The most important implication of the data is that the Γ_i values do satisfy the fracture-mechanical criterion for crack deflection and interface debonding. This criterion states that $\Gamma_i/\Gamma_f < 0.25$, where Γ_f denotes the fracture toughness of the fiber. A typical commercial tungsten wire has Γ_f of about 320 J/m². Substituting the measured Γ_i data together with this Γ_f value into the criterion given above, one finds that the requirement of crack deflection is obviously satisfied ($\Gamma_i/\Gamma_f < 0.25$).

On the other hand, the area below the curves gives an indication of total amount of work done by the applied load. Then the absorbed energy is partly dissipated by plastic flow, fracture and friction and partly stored as elastic strain energy. It is noted that the amount of the work done on the two interface systems was closely comparable with each other. However, this does not

necessarily mean that the both interfaces should have a comparable fracture energy, for the underlying microscopic process could be dissimilar.

The major physical origin of the frictional resistance in the progressive sliding stage can be attributed to the morphological mismatch of the two rough contact faces being created by the interface rupture. The relative motion of the two rough contact faces generates radial stress component as the shear load overcomes the resistance by the asperity in which radial strain is forced. According to Shetty who applied the shear-lag approach to frictional sliding process, the maximum friction load P_{fr} can be correlated with the embedded fiber length l as [13]

$$P_{fr} = \frac{\pi r_f^2 \sigma_r}{k}\left[\exp\left(\frac{2\mu k l}{r_f}\right) - 1\right] \qquad (3)$$

The radial stress σ_r is generated by the roughness (morphological mismatch). k denotes a dimensionless parameter defined by the elastic constants of the fiber and matrix as,

$$k = \frac{E_m \nu_f}{E_f (1+\nu_m)}$$

l equals to the embedded thickness at P_{fr}. σ_r and μ can be determined by fitting the experimentally measured $P_{fr} - l$ data into eq.(3). The roughness induced shear stress τ_r is then obtained from $\mu \times \sigma_r$. The fitting was carried out only for the W/Cu multi-layer coating since the shear-lag model did not consider plastic flow. Results are as follows (see Figure 10): σ_r =123 MPa, μ = 0.81, $\tau_r = \mu \times \sigma_r$ = 99 MPa.

3.3. Microstructure analysis

Figure 11 shows a SEM image of the Cu single-layer coating on the pushed-out wire surface after testing. Several conspicuous features are found in this fractography. First of all, the Cu coating experienced strong plastic deformation extensively. The plastic deformation partly led to shear rupture and local flaking off of the Cu coating from the wire. This fact supports the interpretation that actual debonding occurred at either of the two Cu/W interfaces on the matrix or wire side and even within the copper layer. The locally exposed W-coated surface of the wire showed no residual copper on it indicating clear detachment. While the Cu coating was partly detached from the wire, the main debonding site was the Cu/W interface on the matrix side. Cracks were created at both interface edges as indicated with white arrows. Figure 12 shows the Cu coating in detail. It remained partly attached to the wire and to the matrix. At this position the degree of plastic shear strain seems rather moderate. The amount

of plastic strain is inversely correlated to the bond strength. The cracked interface on the longitudinal cut section is shown in Figure 13. It demonstrates clearly that both of the Cu/W interfaces were debonded whereas the two W/W interfaces remained intact. It should be noted that the two surfaces of the fractured interface are currently in a displaced position from each other and thus not mating with neighboring crack face.

Figure 14 shows the pushed out wire interface of the W/Cu multi-layer coating specimen. The debonding site was obviously one of the Cu layers, preferentially the outermost one. Plastic strain of the Cu layers seems to be quite limited. The cracked interface on the longitudinal cut section is shown in Figure 15. The micrograph exhibits a clearly defined debonding at the outer Cu/W (protection film) interface on the wire side. The internal Cu/W interfaces of the multi-layered coating had apparently larger bond strength. It was also observed that the plastic deformation of the Cu films was strongly suppressed whereas the outermost Cu layer was more or less plastically squeezed. This finding implicates that the contribution of plastic work to the whole push-out work was hardly substantial. This conclusion accords well with the characteristic load-displacement response in Figure 5. In Figure 16 the exposed interface of the ruptured Cu coating (on the fiber side) is shown. Although the apparent overall plastic strain was considerably small, the microscopic fracture pattern of the Cu surface revealed a typical deformation morphology of ductile rupture. Due to the size effect of thin thickness, the rupture elongation of the Cu film normal to the interface was strongly constrained. No shear tearing as found in the Cu single-layer coating was observed.

4. Conclusion

In this work the properties of copper coated fiber/matrix interfaces for a W_w/W composite were successfully investigated using fiber push-out test. Cu single-layer and Cu/W multi-layer coatings were considered for interface engineering. Until the global debonding event at the maximum load, both coatings exhibited nearly identical load-displacement responses. In the frictional sliding stage, however, the two coatings revealed an essentially different energy dissipation behavior from each other. The Cu single-layer coating showed a gradual decrease of load resulting in large push-out work and thus large energy absorption. On the contrary, the Cu/W multi-layer coating demonstrated an apparently brittle push-out response with abrupt load drop as is the case of a ceramic-coated interface. This difference was attributed to the large extent of plastic deformation of the Cu single-layer. The estimated interfacial parameters

implied the potential feasibility of this interface design toward realization of a high toughness tungsten composite material.

Acknowledgement

The authors are grateful to the colleagues of IPP Garching, Dr. A. Brendel, Mr. F. Koch and G. Matern for their support for magnetron sputtering and metallographical preparation. The author Juan Du is also grateful to Chinese Scholarship Council (CSC) for the grant.

Reference

[1] R. Lässer, N. Baluc, J.-L. Boutard, E. Diegele, S. Dudarev, M. Gasparotto, A. Möslang, R. Pippan, B. Riccardi, B. van der Schaaf, Fusion Engng. Des. 82 (2007) 511–520.

[2] M. Faleschini, H. Kreuzer, D. Kiener, R. Pippan, J. Nucl. Mater. 367–370 (2007) 800-805.

[3] H. Kurishita, Y. Amano, S. Kobayashi, K. Nakai, H. Arakawa, Y. Hiraoka, T. Takida, K. Takebe, H. Matsui, J. Nucl. Mater. 367-370 (2007) 1453-1457.

[4] M. Rieth, B. Dafferner, J. Nucl. Mater. 342 (2005) 20-25.

[5] A. G. Evans, Acta Mater. 45 (1997) 23-40.

[6] A. G. Evans, J. Am. Ceram. Soc. 73 (1990) 187-206.

[7] M. Ohring, The materials science of thin films, Academic Press, London, 1992.

[8] L. B. Greszczuk, Interface in Composite, ASTM Special Technical Publication 452, American Society of Testing and Materials, Philadelphia (1969) 42-58.

[9] P. Lawrence, J. Mater. Sci. 7 (1970) 1-6.

[10] C. M. Huang, D. Zhu, X. D. Cong, W. M. Kriven, J. Am. Soc. 80[9] (1997) 2326-2332.

[11] W. D. Zeng, P. W. M. Perters, Y. Tanaka, Composites: Part A 33(2002) 1159-1170.

[12] C. Liang, J. W. Hutchinson, Mech. Mater. 14 (1993) 207-221

[13] D. K. Shetty, J. Am. Ceram. Soc. 71 (1988) C107-C109.

Figure captions

Figure 1. SEM image of the Cu single-layer coated interface together with two W protection films before push-out test. Longitudinal section of the as-fabricated specimen is shown.

Figure 2. SEM image of the Cu/W multi-layer coated interface before push-out test. Longitudinal section of the as-fabricated specimen is shown

Figure 3. Schematic illustration of the push-out testing system.

Figure 4. A typical SEM view of a specimen after push-out test (Cu single-layer coated interface).

Figure 5. Measured push-out load vs. fiber-end displacement curves for the Cu single-layer and the Cu/W multi-layer coated interface. The specimen thickness was 0.248 mm and 0.228 mm, respectively.

Figure 6. Simulated load-displacement response in the initial loading phase predicted by FEM analysis. (Cu single-layer coating interface)

Figure 7. Predicted evolution of the cumulative equivalent plastic strain in the copper single-layer coating. (result of FEM analysis)

Figure 8. Collected debonding load (P_d) data as a function of the specimen thickness (H). Curve fitting result based on the Greszczuk's equation is also plotted for the both interfaces. The calibrated debonding strength was 393 MPa and 429 MPa for the Cu single-layer and Cu/W multi-layer interface, respectively.

Figure 9. Collected maximum applied stress p data as a function of specimen thickness (H). Curve fitting result based on the Liang's equation is also plotted for the Cu/W multi-layer interface. The calibrated interfacial fracture toughness was 22 J/m².

Figure 10. Collected maximum friction load (P_{fr}) data as a function of the embedded fiber length (l). Curve fitting result based on the Shetty's equation is also plotted for the Cu/W multi-layer interface. The calibrated shear stress was 99 MPa.

Figure 11. Cu single-layer coating on the pushed-out wire surface after testing (SEM image).

Figure 12. Local view of the Cu single-layer coating partly attached to the pushed-out wire surface and partly to the matrix side (SEM image).

Figure 13. Cracked Cu single-layer coating interface on the longitudinal cut section after testing (SEM image).

Figure 14. Pushed out wire interface of the W/Cu multi-layer coating specimen (SEM image).

Figure 15. Cracked Cu/W multi-layer coating interface on the longitudinal cut section after testing (SEM image).

Figure 16. Exposed surface of the ruptured outermost Cu film of the W/Cu multi-layer coating (SEM image).

Figure1

Click here to download high resolution image

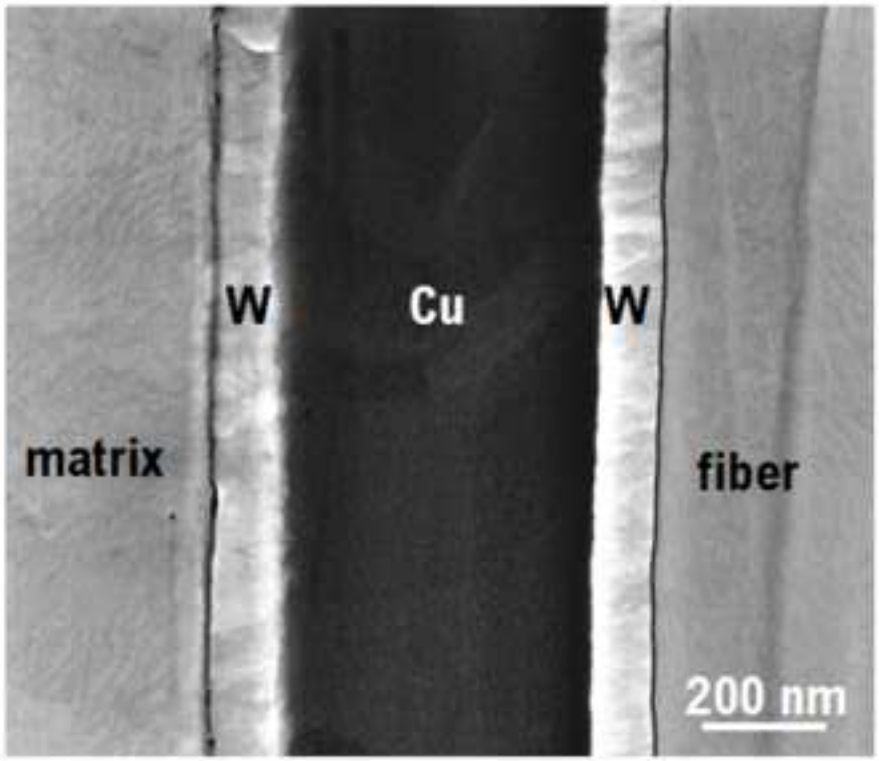

Figure2

Click here to download high resolution image

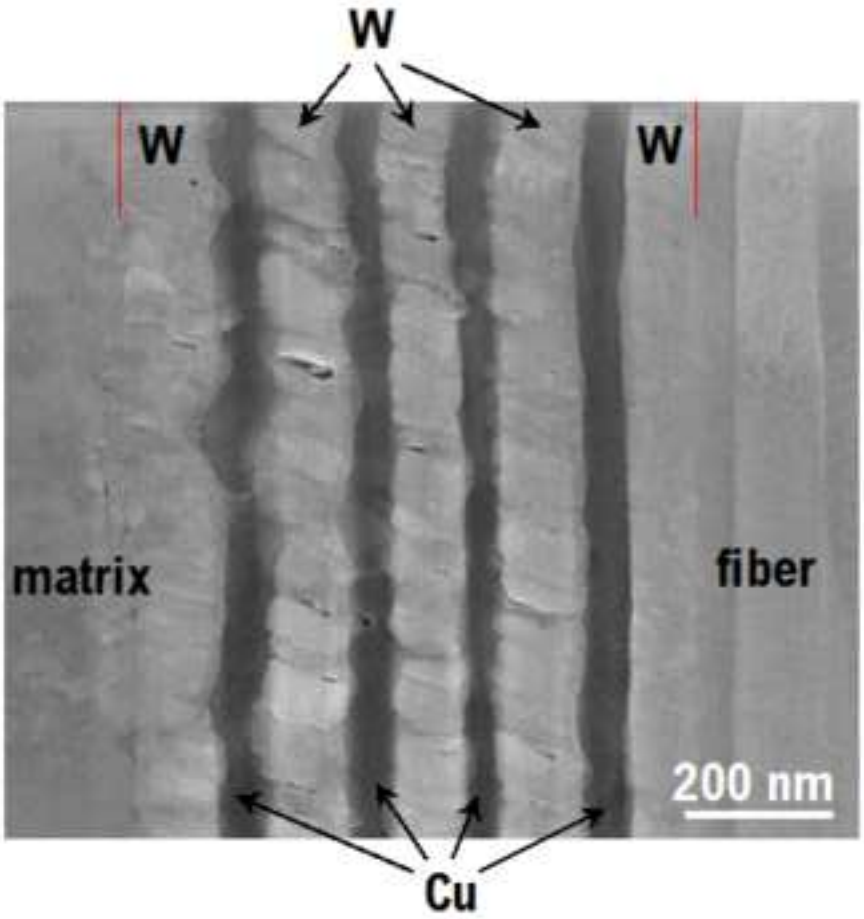

Figure3

Click here to download high resolution image

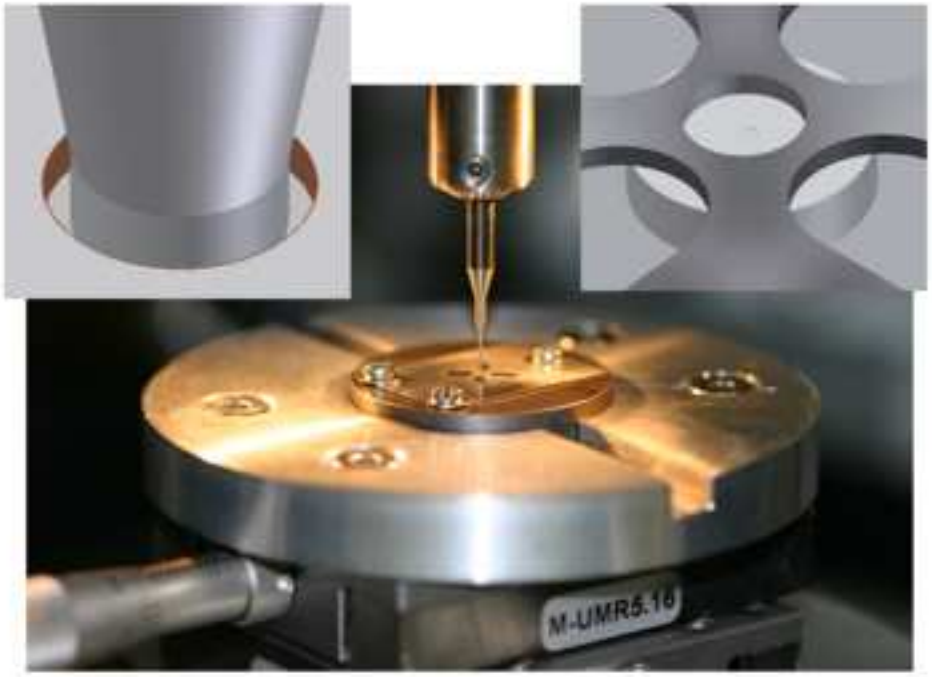

Figure4

Click here to download high resolution image

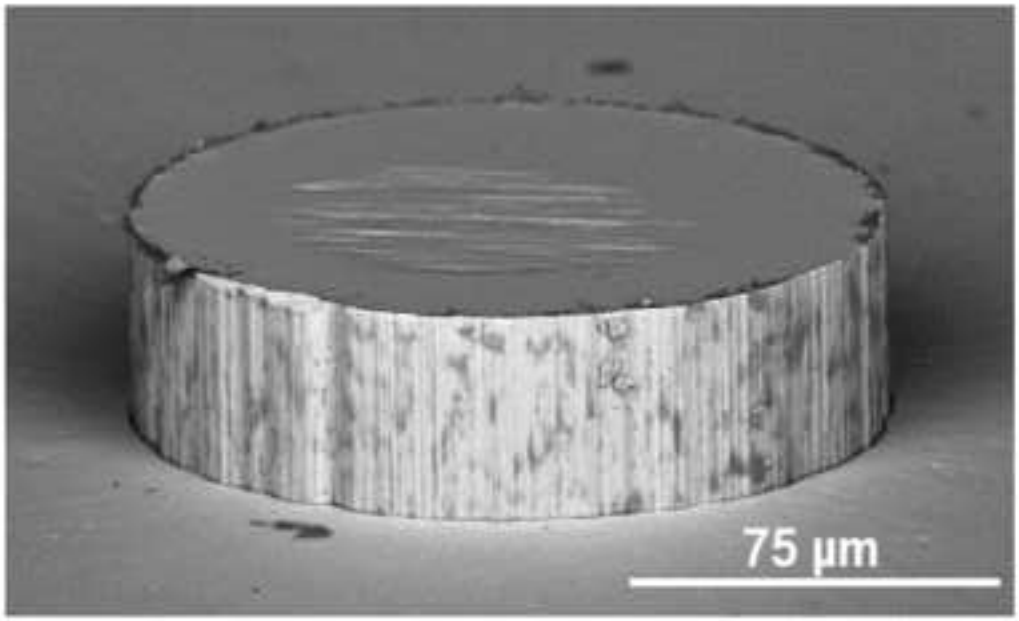

Figure5

Figure 5. Measured push-out load vs. fiber-end displacement curves for the Cu mono-layer and the Cu/W multi-layer coated interface. The specimen thickness was 0.248 mm and 0.228 mm, respectively.

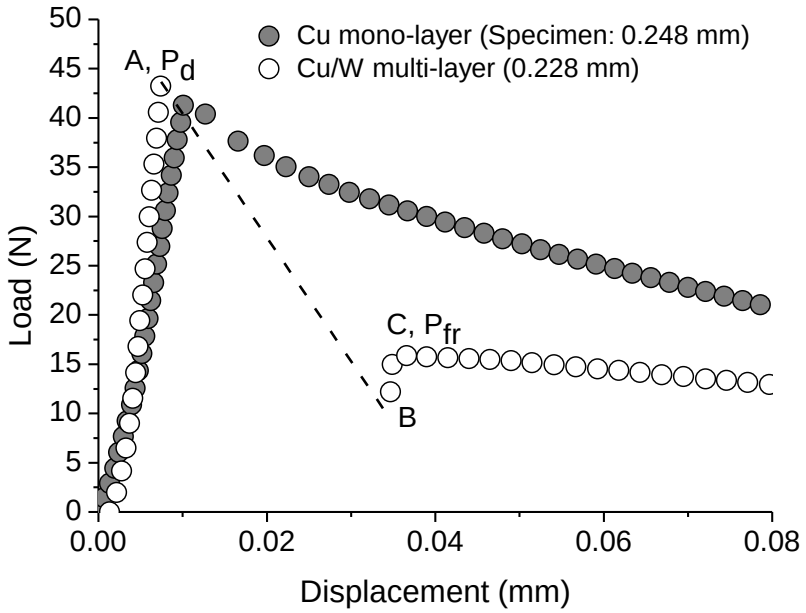

Figure6

Figure 6. Simulated load-displacement response in the initial loading phase predicted by FEM analysis. (Cu mono-layer coating interface)

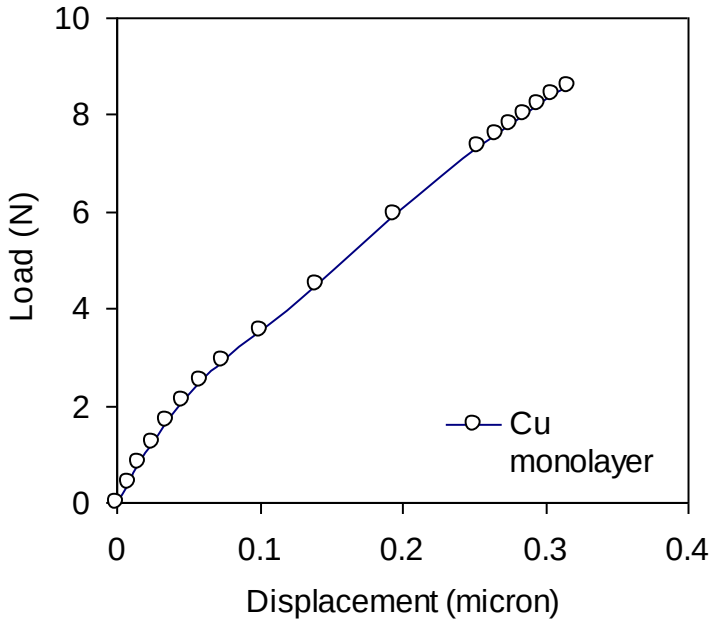

Figure7

Figure 7. Predicted evolution of the cumulative equivalent plastic strain in the copper mono-layer coating. (result of FEM analysis)

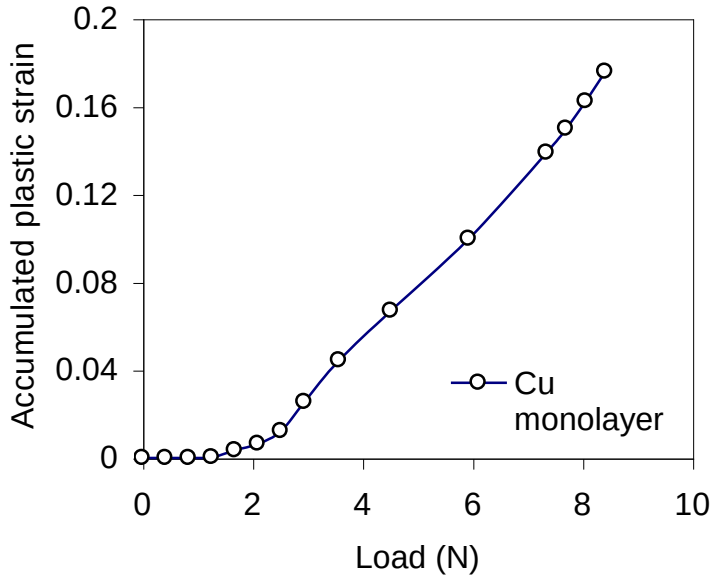

Figure8

Figure 8. Collected debonding load (P_d) data as a function of the specimen thickness (H). Curve fitting result based on the Greszczuk's equation is also plotted for the both interfaces. The calibrated debonding strength was 393 MPa and 429 MPa for the Cu mono-layer and Cu/W multi-layer interface, respectively.

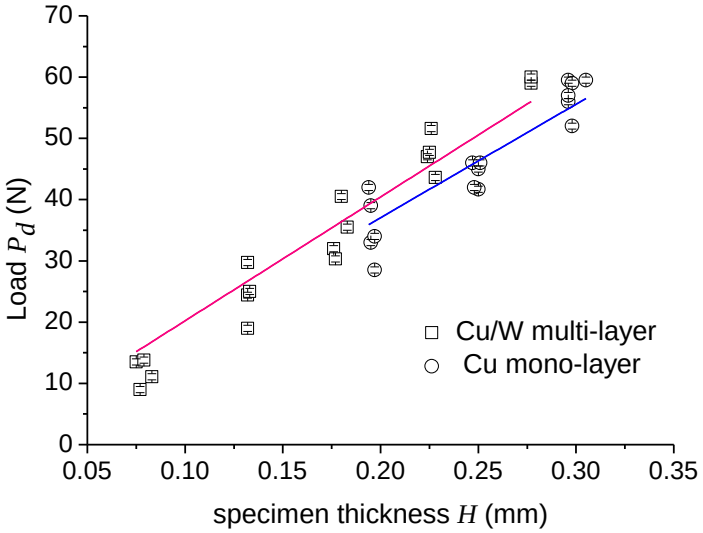

Figure9

Figure 9. Collected maximum applied stress p data as a function of specimen thickness (H). Curve fitting result based on the Liang's equation is also plotted for the Cu/W multi-layer interface. The calibrated interfacial fracture toughness was 22 J/m².

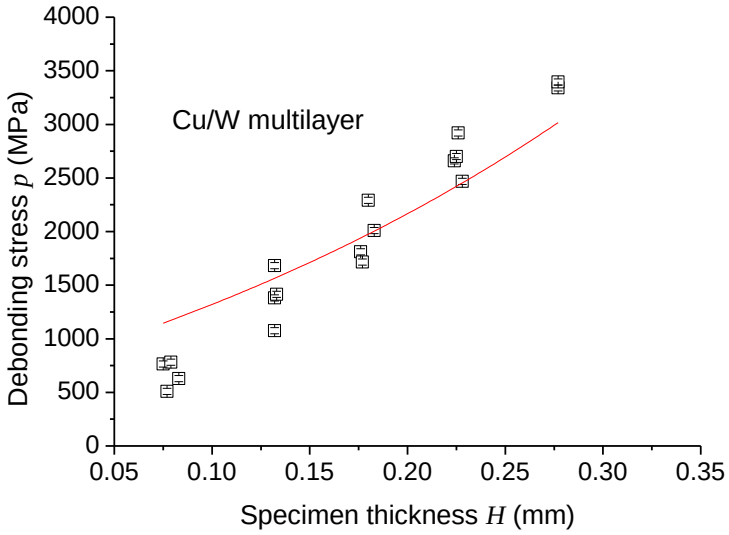

Figure10

Figure 10. Collected maximum friction load (P_{fr}) data as a function of the embedded fiber length (l). Curve fitting result based on the Shetty's equation is also plotted for the Cu/W multi-layer interface. The calibrated shear stress was 99 MPa.

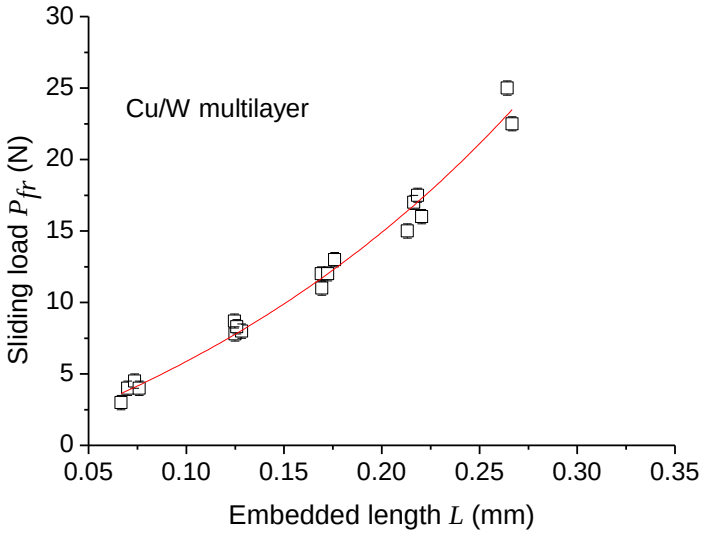

Figure11

Click here to download high resolution image

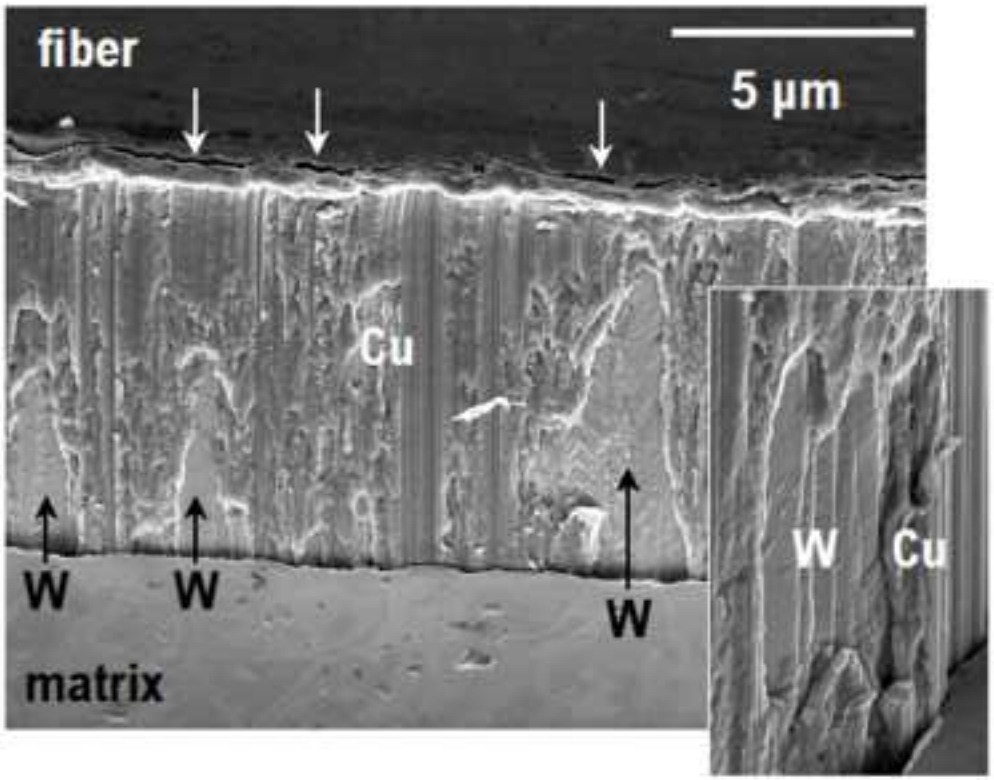

Figure12

Click here to download high resolution image

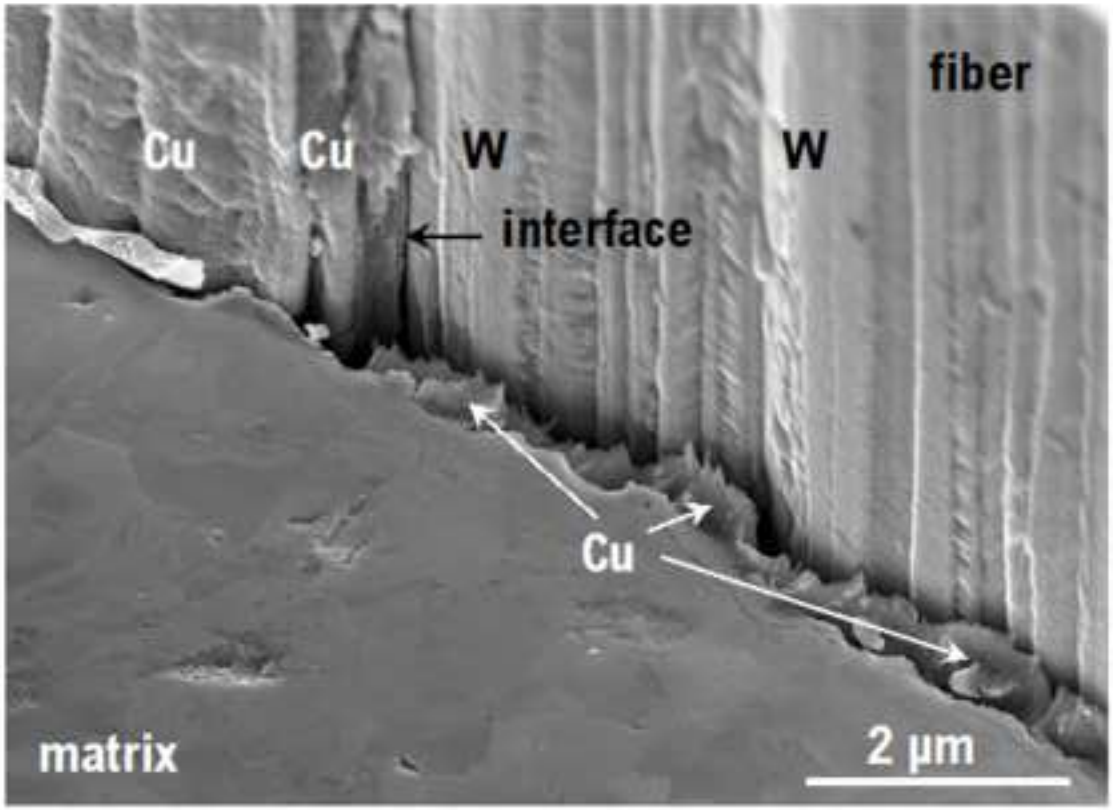

Figure13
Click here to download high resolution image

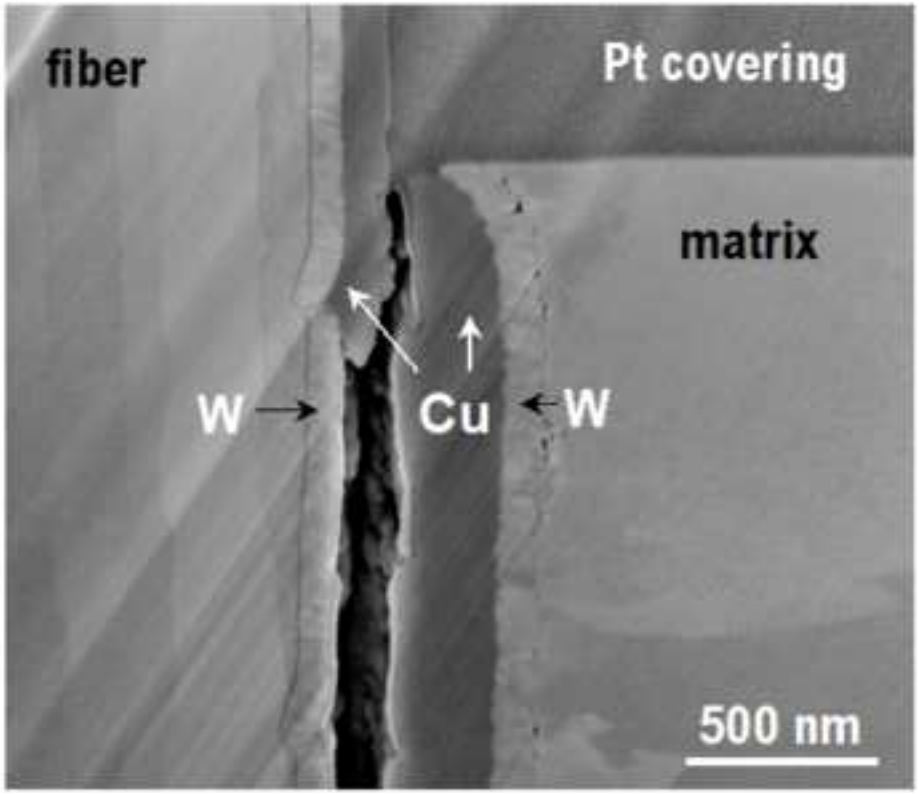

Figure14

Click here to download high resolution image

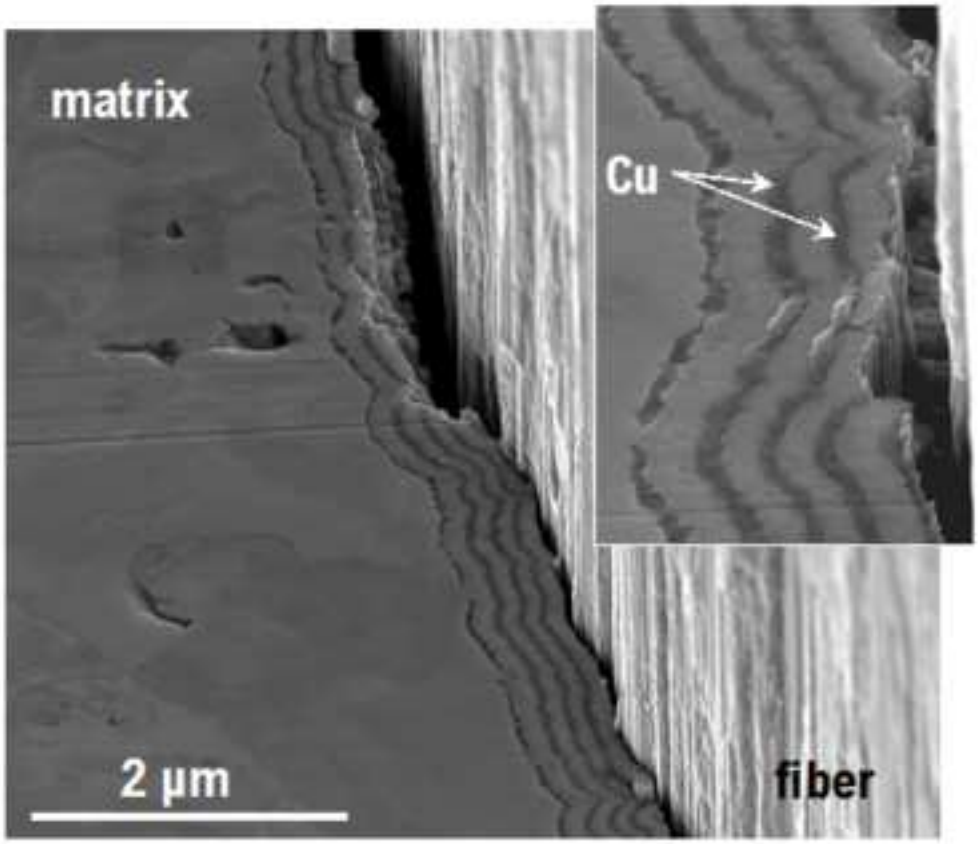

Figure15

Click here to download high resolution image

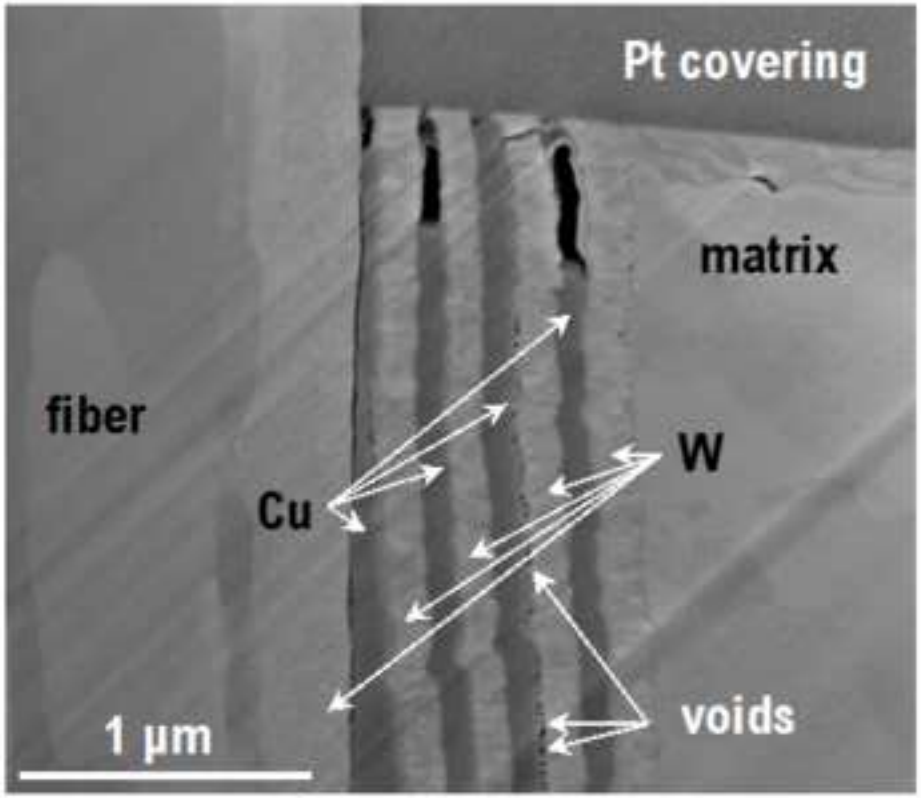

Figure16

Click here to download high resolution image